Journal of The Electrochemical Society, **155** (4) C147-C153 (2008)
0013-4651/2008/155(4)/C147/7/$23.00 © The Electrochemical Society

Study of Mixed Flowing Gas Exposure of Copper

M. Reid,[a,*,z] J. Punch,[a,z] L. F. Garfias-Mesias,[d,*,z] K. Shannon,[e,z] S. Belochapkine,[b,z] and D. A. Tanner[c,*,z]

[a]*CTVR, Stokes Institute,* [b]*Materials and Surface Science Institute,* [c]*and Department of Manufacturing & Operations Engineering, University of Limerick, Limerick, Ireland*
[d]*DNV-CC Technologies, Corrosion and Materials Technology Laboratory, Dublin, Ohio 43017-1386, USA*
[e]*Southwest Research Institute, San Antonio, Texas 78238, USA*

This paper describes the results of copper coupons exposed to a class III mixed flowing gas environment (MFG) following the guidelines given by the Battelle Laboratory and the International Electrotechnical Commission for environmental testing. Corrosion products were studied in detail using scanning electron microscope, energy dispersive X-ray spectroscopy (EDS), X-ray diffraction (XRD), focused ion beam (FIB), secondary ion mass spectroscopy (SIMS), and transmission electron microscope. The weight gain measured after each exposure was compared with the weight gain calculated from the cathodic reduction of the corrosion layers and cross sectioning using an FIB. The result shows a relatively good correlation between the measured and the calculated experimental values of weight gain. As expected, within the first week, the different corrosion layers thickened until they formed a thick layer that became the determining step for further growth. After several days of exposure the Cu coupons developed a complex multilayered structure consisting of cuprous oxide (Cu_2S), cupric oxide (CuO), copper sulfide (Cu_2S), covellite (CuS), and evidence of antlerite ($3CuO\ SO_3\ 2H_2O$). No Cl-containing corrosion products were identified using XRD. However, EDS and SIMS analysis showed that Cl was distributed throughout the corrosion products, indicating that although Cl is inside the corrosion products, it is not part of the crystalline structure. Also, this suggests that Cl plays an important role in accelerating the corrosion of Cu during exposure to the MFG class III test.
 [DOI: 10.1149/1.2837834]

Manuscript submitted June 20, 2007; revised manuscript received November 27, 2007. Available electronically February 12, 2008.

In the early 1980s, with the discovery of significant printed wiring board (PWB) and component failure modes (mainly due to corrosion), a number of firms and laboratories set out to develop accelerated corrosion test methods with a known acceleration factor. The aim of such efforts was to shrink years of service into days of testing, and prove that the field failure modes would be replicated during the tests. The PWB and its components were exposed to different levels of a mixture of gases, temperature, and relative humidity, which would simulate the environment during operating conditions. IBM, AT&T, and Battelle Laboratories participated in this effort.[1] The result of this work was the development of a mixed flowing gas (MFG) test, which is primarily a laboratory test in which the temperature, relative humidity, and concentration of gaseous pollutants are carefully defined, monitored, and controlled.[1-4] Based on the weight gain and thickness of corrosion products of copper coupons, a set of environmental corrosion classes was defined by the group to allow comparisons among field locations and test conditions within the chambers.[1,2] Table I summarizes the nominal test conditions for standard MFG exposure, ranked in order of severity. The class I environment corresponds to a benign environment in which the corrosion film of Cu in one year will not exceed 35 nm. Class II is a mild corrosive environment (i.e., a rural environment), in which the corrosion film of Cu in one year should be between 40 and 70 nm. Class III is a harsh corrosive environment (i.e., populated urban environment) in which the corrosion film of Cu in one year would be between 80 and 400 nm. Finally, class IV is a severe corrosive environment (i.e., harsh industrial environment) where the corrosion film of Cu would exceed 500 nm in one year.

During the decade of the 1990s professional organizations, including the American Society for Testing and Material, Electronic Industries Association, International Electrotechnical Commission (IEC), and Telcordia, began to standardize these test methods and published corresponding documents as guidelines.[3,4] The standards developed were for equipment deployed in the North America Region (NAR) and are considered to provide accelerated aging conditions for NAR and Europe-type environments only. To the best of our knowledge, no comprehensive studies have been undertaken in order to identify the corrosion products formed on Cu during MFG class III testing, although numerous authors have studied the effect of MFG exposure on different electronic components.[5-11] Therefore, this paper will focus on a detailed investigation of the corrosion products that develop on Cu after prolonged exposure to class III MFG. The test conditions used follow the guidelines given by Battelle and IEC for environmental testing.[3,4]

Experimental

The MFG test was performed in an exposure chamber over 20 days with removal of triplicate samples after 1, 2, 3, 4, 5, 7, 10, 15, and 20 days. The chamber was designed to provide an environment with controlled temperature, humidity, gas concentration, and volume exchange rate. Figure 1 shows a schematic illustration of the environmental exposure chamber (Southwest Research Institute). A dry compressor with in situ filters provided the system with purified dry air. The main dry air gas flow passed the humidifier on its way to the test chamber. Before entering the exposure chamber the humidified air was mixed with dry corrosive gases flowing into the chamber (H_2S, NO_2, SO_2, and Cl_2), which were supplied from bottled gas sources. The exposure chamber was comprised of an acrylic box ($1.8 \times 1.8 \times 1$ m) with the gas inlet near the bottom of the chamber and the exhaust near the top. The exposure chamber had a volume exchange of 6.9 times per hour, a volumetric flow rate of 350 L/min, yielding a mean local velocity within the chamber of order 3.5 mm/s. Four fans were also strategically placed in the chamber to ensure a uniform gas flow. According to the MFG test guidelines, exposure can be performed in chambers with either high or low exchange rates. High exchange rate chambers operating at greater than 30 times per hour have the capability to expose larger Cu samples and equipment with a large number of electronic devices. However, higher air exchange rates are more difficult to maintain at the specified concentration. Furthermore, the mixture of pollutants has to be disposed, with the resulting effect on the environment. We feel that, because of the very low surface area exposed on the coupons and in order to maintain a reasonable critical concentration, a low air exchange rate (6.9 times per hour) was sufficient for these experiments. By calculating a mixing ratio between the dry air and wet gas flow, the humidifier allowed control of

* Electrochemical Society Active Member.
z E-mail: michael.reid@ul.ie; jeff.punch@ul.ie; luis.garfias@dnv.com; kevin.shannon@swri.org; serguei.belochapkine@ul.ie; david.tanner@ul.ie

Table I. Nominal test conditions for standard MFG exposure.

Class	H_2S (ppb)	Cl_2 (ppb)	NO_2 (ppb)	SO_2 (ppb)	% RH	T(°C)
I	-	-	-	-	-	-
II	10	10	200	200	70	30
III	100	20	200	200	70	30
IV	200	50	200	200	75	50

the relative humidity, which was continuously monitored by a calibrated Vaisala HMP233 temperature and humidity transmitter. The concentrations of the NO_2, SO_2, and H_2S were monitored by Teledyne-API Instruments models M200E, M100E, and M101E, respectively. The Cl_2 concentration was monitored using impingers for air sampling over 8 h, then analyzed by ion chromatography. After correct values were achieved the mass flow controller connected to the source cylinder was set and continually monitored.

Pure Cu coupons (99.99%) 12 × 12 mm and 0.6 mm thick were used as the substrate material for this study. Prior to MFG exposure, the test specimens were sonicated in deionized water followed by a soak in hydrochloric acid solution, then rinsed in distilled water, and subsequently dried with dry oxygen-free nitrogen gas. Following cleaning, energy-dispersive X-ray (EDS) on a sample showed no evidence of any containment, indicating a successful cleaning procedure. After this initial preparation, the samples were weighed with an electronic balance (1 μg accuracy). Triplicate samples were removed from the exposure chamber at set times and weighed immediately after removal from the chamber.

A Philips X'Pert X-ray diffraction (XRD) system with Ni filtered Cu Kα radiation (λ = 1.54056 nm) was used to obtain diffractograms over a 2θ range of 20–90° with a scan speed of 0.017° 2θ s^{-1}. A focused ion beam (FIB) microscope FEI 200 was used to obtain cross sections. A JEOL JSM-840 scanning electron microscope equipped with a Princeton Gamma-Tech EDS system was used to obtain chemical composition and imaging on the surface of the coupons. Secondary ion mass spectroscopy (SIMS) was used to obtain mass spectra and depth profiling, showing the chemical composition of the film at the surface and deep within the boundaries of the different corrosion layers. A scan area of 25 μm^2 was used and gated to 50%. Secondary ions were detected as positive and negative ions. SIMS depth profiling through the oxide was conducted in close vicinity to the FIB cross-section analysis in order to draw a correlation with the distribution of trace elements as a function of depth.

Transmission electron microscopy (TEM) measurements were acquired for corrosion products on carbon-coated Ni TEM grids [JEM-2011, JEOL UK Ltd.; Gatan DualVision 600 charged-coupled detector camera and digital micrograph software, Gatan UK Ltd.]. The corrosion products were removed from the corroded Cu coupons by a diamond scraper and then deposited on the carbon-coated Ni TEM grids. Selected area electron diffraction (SAED) patterns were recorded from representative areas of the sample with a camera length of 33.5 cm. The TEM was calibrated using standard samples both for magnification and diffraction.

One coupon from each exposure time was selected for electrochemical reduction using a PARSTAT 2273 advanced electrochemical system (Princeton Applied Research). The electrochemical cell was fitted with high-density graphite rods as the counter electrode and the potentials measured with reference to a saturated calomel electrode. The selected electrolyte was a potassium chloride solution 0.1 M which was carefully purged with nitrogen before each run.

Results and Discussion

Figure 2 shows the mass gain per unit surface area as a function of time for Cu coupons exposed for 20 days to MFG class III. The plot exhibits a typical behavior for a corrosion process with a cohesive product layer. During the first 7 days of exposure, the thickness of the corrosion film increased linearly, followed by a slowdown, suggesting a transition from activation control (where the determining step is the reaction of the corrosive species with the Cu) to diffusion control (where the diffusion of the species through the corrosive layer is more important).[12,13] After the slowdown behavior, an additional slower rate of linear growth (slower than the first week) was observed, possibly indicating a combination of activation and diffusion control.

Figure 3 shows a typical cathodic reduction curve for one Cu coupon exposed for 2 days. There are three reduction plateaus in this graph, I, II, and III, which are related to the reduction reaction of the different layers of corrosion products (the reduction part of the curve). There are conflicting views regarding the order of reduction of Cu corrosion products, in particular Cu oxides.[14-17] However, convincing evidence presented by Nakayama et al., on differently prepared samples of Cu oxide films, demonstrated that CuO (plateau I) is first reduced in 0.1 M KCl, followed by the reduction of cuprous oxide (Cu_2O) (plateau II).[18] The reduction of the Cu_2O is additionally complicated by the reduction of covellite (CuS), which occurs in the potential region of Cu_2O (plateau II). Due to the closeness of the reduction potentials of the corrosion products, an overlap between the reductions of the different corrosion products was observed, resulting in less-defined steps.[17,18] In order to distinguish the

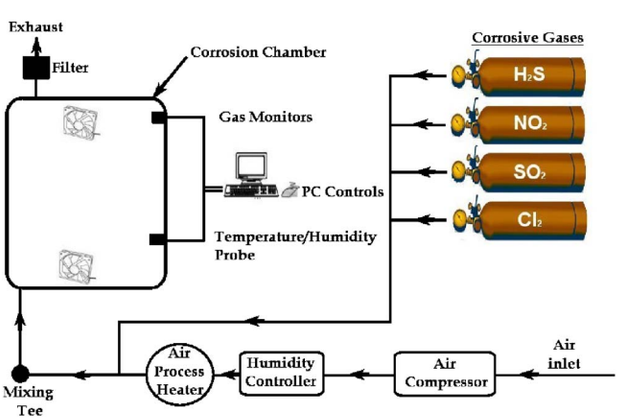

Figure 1. (Color online) Schematic diagram of the MFG test chamber setup.

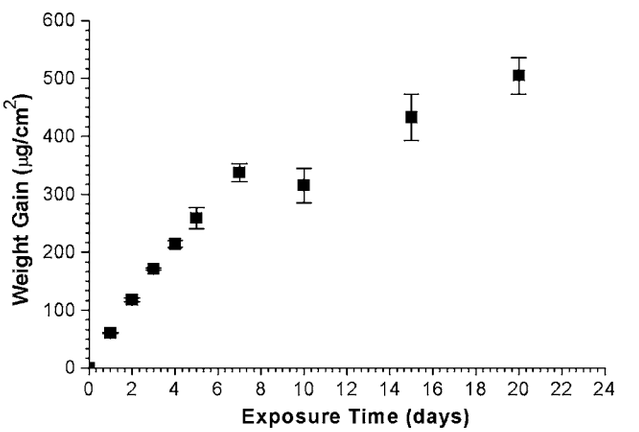

Figure 2. Mass gain vs time for Cu exposed to class III MFG.

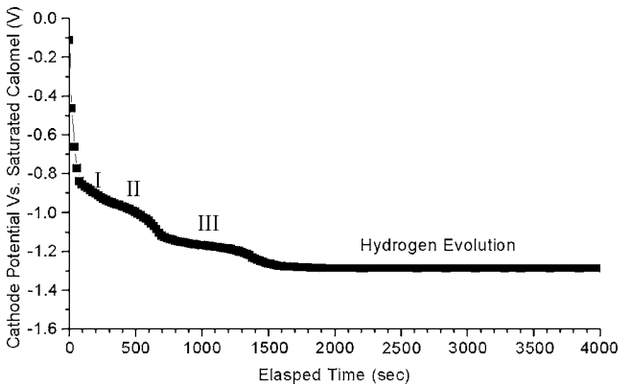

Figure 3. Cathodic reduction curve for Cu exposed for 2 day in class III MFG.

different reduction potentials, the approximate midpoints of the differential maxima for the beginning and end of a particular reduction arrest were estimated by measurement.[17] The obtained reduction peaks for Cu_2O and CuS showed an insufficient separation, and a conclusive verification was therefore not obtained in all cathodic reduction curves. Finally, plateau III corresponds to the cathodic reduction of the copper sulfide (Cu_2S), with the hydrogen reduction potential represented by the last portion of the reduction curve. For simplicity, plateau II was assumed to correspond to the cathodic reduction of Cu_2O. The overall thickness of the corrosion products was calculated in accordance with the following equation[17]

$$T = \frac{10^4\ Mit}{\rho nF} \qquad [1]$$

where T is film thickness (nm), M is the molecular weight of the compound, i is current density (mA/cm^2), t is the elapsed time required to reduce a film (s), ρ is the density of a film (g/cm^3), n is the equivalent per gram atom of the film, and F is Faraday's constant. Figure 4 shows the calculated thickness of the corrosion films as a function of exposure time; the total film thickness was obtained by adding the thickness calculated for each of the reduced corrosion products. After 1 day exposure, a significant increase in thickness was observed, followed by a linear increase up to 7 days exposure. Between 7 and 10 days exposure a slowdown in the formation of corrosion products was observed. Finally, after 10 days exposure a significant drop in the corrosion product thickness was observed. During the entire duration of the experiment Cu_2O was observed;

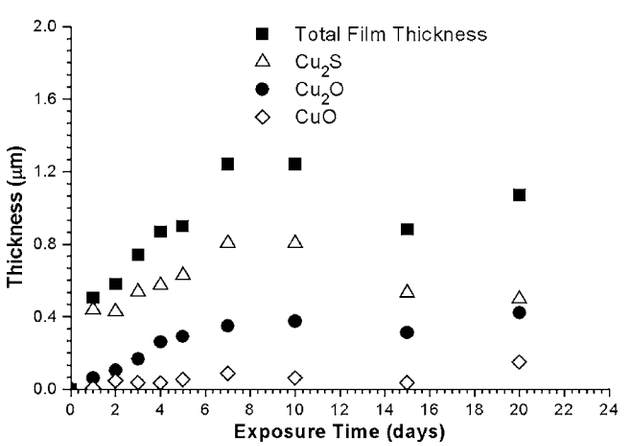

Figure 4. Calculated variation of corrosion layer thickness from cathodic reduction of Cu during exposure to class III MFG.

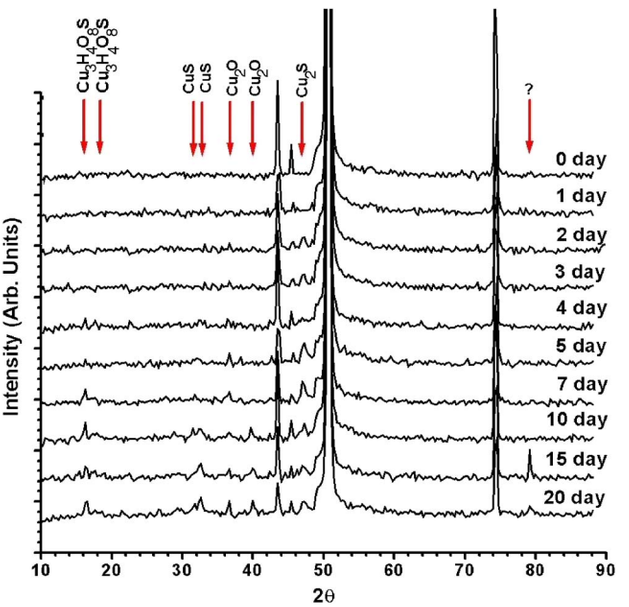

Figure 5. (Color online) X-ray diffractometer traces observed from Cu exposed for 0, 1, 2, 3, 4, 5, 7, 10, 15, and 20 days in class III MFG.

however, the main corrosion product was Cu_2S. CuO was observed, although only as a minor constituent in the corrosion film.

The XRD spectra for all the samples exposed to different times are illustrated in Fig. 5. After 1 day exposure only the peaks corresponding to Cu were observed. No peaks corresponding to any corrosion products were observed. This most likely indicates that a very thin layer of corrosion products had formed, which is probably beyond the detection limit of the X-ray diffractometer. After 2 days of exposure, small peaks corresponding to Cu_2O and Cu_2S started to appear in the X-ray traces, demonstrating that the corrosion layers correspond to a combination of Cu_2O and Cu_2S. After a more prolonged exposure, the peaks related to the different products were more clearly visible, including the peak corresponding to antlerite ($3CuO\ SO_3\ 2H_2O$). No peaks corresponding to CuO were observed, despite evidence of CuO after cathodic reduction. The limited dimensions of the CuO film would indicate that the film was too thin to be detected by XRD.

In order to investigate the structure of the 1 day exposed sample, the corrosion product was scraped onto a carbon-coated solid Ni TEM grid for TEM analysis. Figures 6a and b show a TEM image of the scraped corrosion product with an SAED pattern inserted in the bottom right of the image and an EDS spectrum, respectively. The electron diffraction pattern shows excellent agreement for d-spacing corresponding to the hexagonal structure of Cu_2S (JCPDS 46–1195). The EDS spectrum in Fig. 6b reveals the presence of Cu, S, Cl, and Ni (Ni can be attributed to the Ni grid from the sample holder). Oxygen was not detected, as it cannot be routinely detected by EDS because only elements of the atomic number of Na or greater release sufficient X-rays; also, scraping of the corrosion product does not allow determination of EDS analysis on a specific location of the corrosion film, i.e., the top surface.

The images depicted in Fig. 7a-h shows FIB cross sections of the corrosion film formed on the copper substrate after exposure for 1, 2, 3, 4, 5, 7, 10, and 15 days, respectively. FIB cross sections were conducted on numerous sites on each sample in order to get an overall picture of corrosion layer development. Due to the level of flaking observed after 20 days, it was not possible to conduct cross sections due to the redeposition of sputtered layers during milling.

Figure 7a shows that after 1 day exposure, the corrosion film was thin (approximately 100 nm). The corrosion film after 2 and 3 days

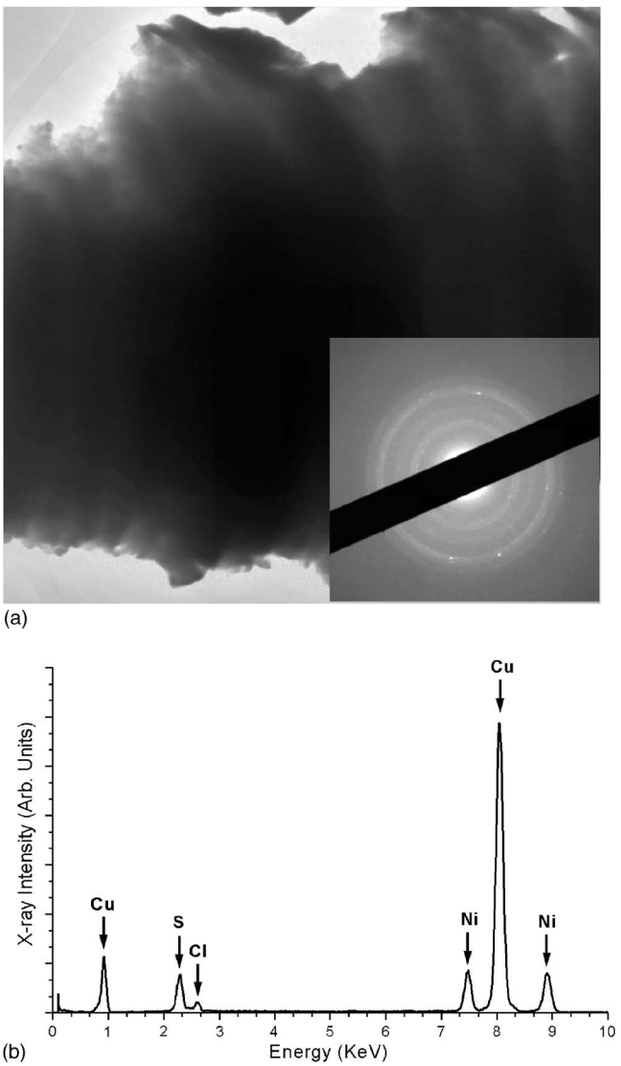

Figure 6. (a) TEM image with its corresponding SAED pattern. (b) EDS spectrum on corrosion product after 1 day class III MFG.

was very similar, approximately 525 nm. On day 4 the corrosion layer was close to 600 nm. On day 5 the corrosion layer was relatively uniform in thickness and structure and close to 800 nm. After 5 and 7 days exposure a two-layered structure was observed (see Fig. 7e and f). At 10 and 15 days exposure a more complex multilayered structure was observed. Figures 7g and h show that the top layer is not adhered well to the underlying layers and is quite porous in structure, allowing the transport of gases and water to accelerate the further oxidation and sulfidation of the underlying Cu substrate.

The image depicted in Fig. 8 shows the total thickness of the corrosion film measured by FIB cross section as a function of exposure time. The corrosion film appeared to increase linearly over the first 10 days of exposure, followed by a slowdown, again suggesting a transition from activation control to diffusion control.

The calculated cathodic reduction corrosion layer thickness in Fig. 4 shows some disparity with the FIB cross-section thickness measurements in Fig. 8. The thickness determined by cathodic reduction for the samples exposed for 1–4 days inclusive showed a thicker corrosion film than that measured by the FIB cross sections. After 5 and 7 days exposure the FIB cross-section thickness measurements showed a good agreement with the cathodic reduction calculations. However, after 10 days exposure the corrosion product thickness values determined by cathodic reduction showed a significant drop in thickness in comparison to the FIB cross-section measurements. The discrepancies between the FIB cross-section thickness measurements and the calculated cathodic reduction thickness may be attributed to a number of factors: First, variations in the corrosion product thickness caused by localized differences (and stress), particularly around the coupon edges, which were not taken into account in the FIB cross-section measurements where local sections were studied on the sample surface. Second, in an attempt to compare the different corrosion products and film thicknesses after different exposure times, one current density value ($0.35\ mA/cm^2$) was chosen. This relatively high current density may have attributed to the film reduction proceeding at an unreasonable rate, especially after 1 day where a thinner film was clearly evident from the XRD and FIB results. Finally, due to flaking of the corrosion product after 10, 15, and 20 days exposure, it was not possible to fully reduce the entire corrosion product. Cathodic reduction quantifies the electricity required for the reduction of different corrosion products, which is not possible if it is not in electrical contact with the substrate. This is also complicated by the fact that the corrosion products with the lowest reduction potentials are reduced first. In this case CuO is reduced first followed by Cu_2O, CuS, and finally Cu_2S.[17] As copper has a naturally thin oxide film on its surface, therefore it is reasonable to assume that for thicker films with a multilayered structure, the reduction of the inner Cu oxides will invariably be reduced first. This may reduce the stability of CuS and Cu_2S layers and may cause unnecessary flaking; also, this effect is more likely to be more pronounced after more prolonged exposure where the corrosion products are thicker.

Figure 9 shows a plot of the weight gain of Cu measured in each of the three coupons (Fig. 2) compared with the weight gain calculated from both the cathodic reduction and FIB cross sections. Notice that, in the case of the cathodic reduction, the calculations use the thickness of each layer. In the case of the FIB cross sections, the weight gain is calculated assuming a $5.8\ g/cm^3$ density for this oxide (which is a midpoint for the densities of Cu_2O and Cu_2S, which are the main components of the corrosion layer). Even though the corrosion films are complex in nature (as described above) and assuming that the corrosion layers are about 50% porous, it is possible to obtain a good correlation between the measured weight gain and the calculated values.

Figures 10a-d show the SIMS depth profile studies of Cu, O, S, and Cl, respectively, after 1, 2, 5, and 10 days exposure. As mentioned previously, the corrosion film after 1 day exposure was relatively thin in comparison to the films after more prolonged exposure. The Cu intensity after 1 day exposure (the black line in Fig. 10a) demonstrates a steady-state relationship with a sputtering time up to approximately 30 s, increases before the Cu surface, and decreases sharply at approximately 35 s. The intensity of O (the black line in Fig. 10b) gradually increases with sputtering and spikes before coming near the Cu surface, followed by a sharp decrease at approximately 35 s. The corresponding increase of Cu and O near the Cu surface would indicate the presence of copper oxide at the surface. The intensity of the Cu and O profiles near the surface broadens with increasing the exposure time, indicating an increase in the oxide thickness, which is consistent with the calculated thickness of the Cu_2O layer in Fig. 4. Previous studies on the composition and structure of copper films exposed to ambient air showed that copper reacts to form a thin Cu_2O layer approximately 1.6 nm thick, covered by an adsorbed water/hydroxyl layer with hydrocarbon approximately 0.8 nm thick.[19] The S distribution in the corrosion films exposed to different times before 10 days exposure was generally distributed throughout the corrosion layer, but even more so in the upper part of the corrosion film (Fig. 10c). After 10 days exposure the S intensity near the surface dropped considerably when compared to samples exposed to 1, 2, and 5 days. This is in good agreement with the FIB cross sections (Fig. 7g and h), where a clearly different corrosion layer was present at the surface. XRD results showed earlier that this outer layer may indicate the formation of antlerite at around 10 days exposure. Antlerite is mainly

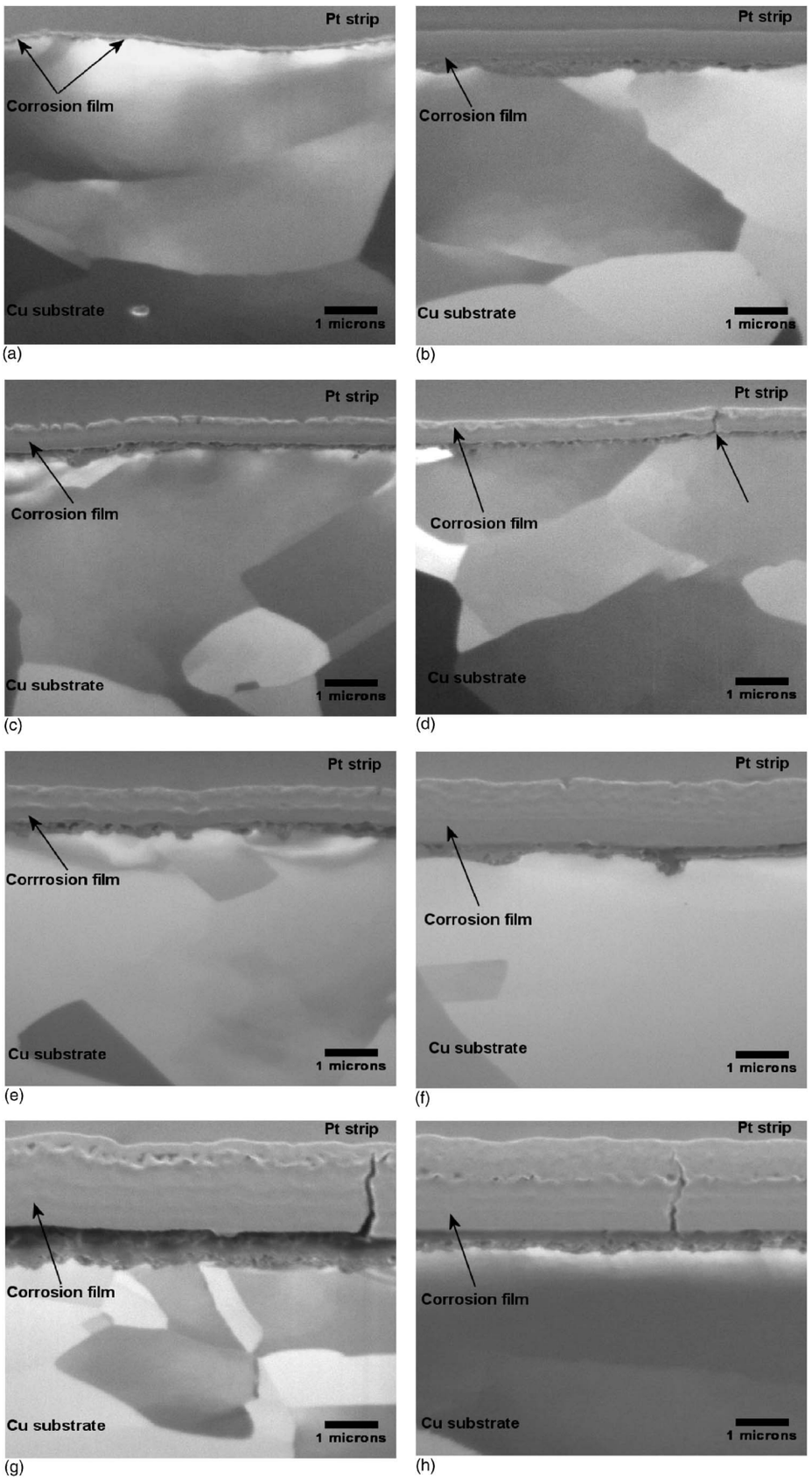

Figure 7. FIB-generated cross sections of Cu exposed to class III MFG for (a) 1, (b) 2, (c) 3, (d) 4, (e) 5, (f) 7, (g) 10, and (h) 15 days.

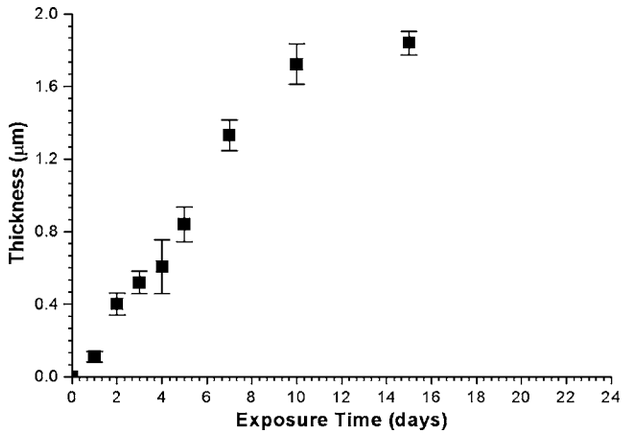

Figure 8. FIB cross-section measurements of corrosion layer thickness of Cu during exposure to class III MFG.

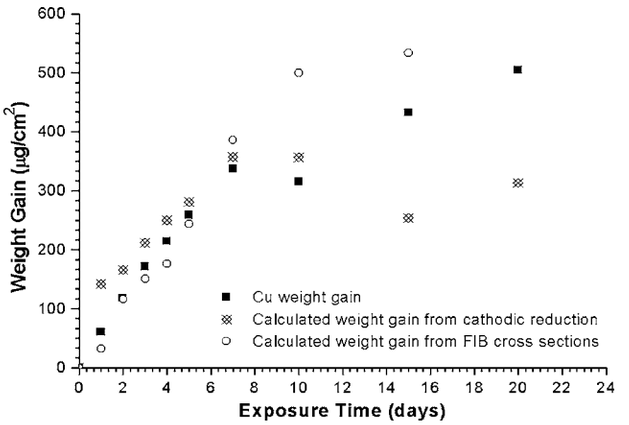

Figure 9. Weight gain as a function of time for Cu samples exposed to MFG III environment. Comparison of the weight gain measured in the Cu coupons after exposure with the weight gain calculated using the data from cathodic reduction and cross sectioning using the FIB.

found in sheltered areas that have been exposed to the outdoor environment for extended periods. The lack of evidence for antlerite in rain-washed areas was suggested to be due to the slow kinetics of formation.[20] The slowdown in growth observed after 7 days exposure may suggest that antlerite has the opportunity to form and explain why it was observed after 10 days exposure.

During the initial rate of growth over the first 7 days, the linear increase of the thickness of the corrosion films with time showed that diffusion is not a rate-limiting parameter. The sulfidation and oxidation processes began on Cu_2O. Cu_2S grew laterally across the initial layer until it joined into a continuous film. Diffusion now had to occur through the Cu oxide layer and through the Cu_2S layer. When the thickness of the films reached a value of approximately 1.2 μm, the rate of the film growth became parabolic, mainly be-

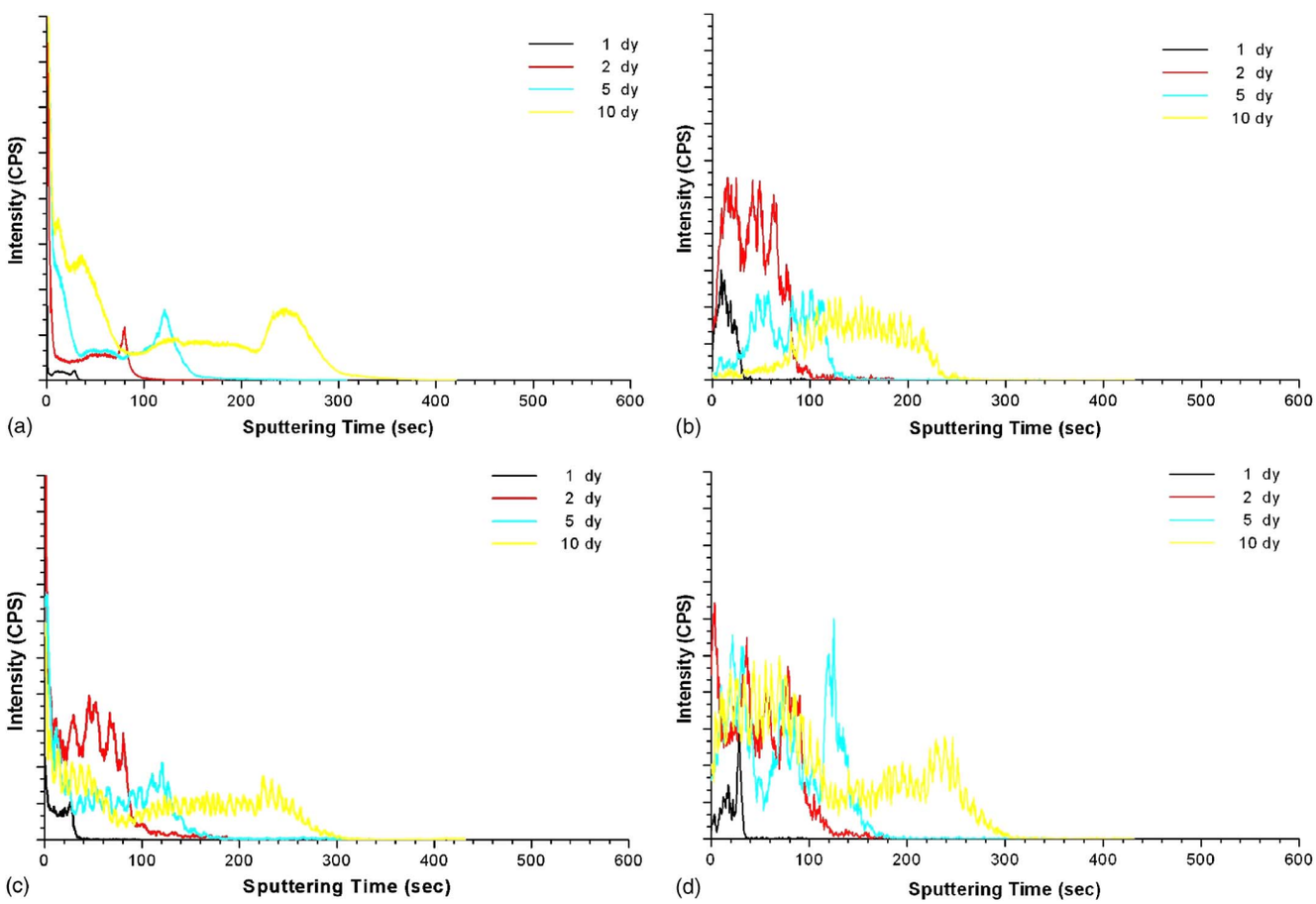

Figure 10. (Color online) SIMS depth profile of (a) Cu, (b) O, (c) S, and (d) Cl after 1, 2, 5, and 10 days in class III MFG.

cause the diffusion of Cu through the thicker corrosion layers is the rate-limiting step. At this critical thickness, the internal stress and defects in the corrosion layer allowed access of corrosive gases and humidity to the underlying layers; as a consequence, accelerated linear growth was observed after the parabolic behavior.

Surprisingly, no Cl-containing corrosion products such as Atacamite [$Cu_2Cl\ (OH)_3$] and Nantokite (CuCl) were detected by XRD or cathodic reduction. However, SIMS depth profiles (Fig. 10d) clearly show that the Cl penetrated the entire corrosion film. Similar observations have been made by Watanabe et al., who characterized corrosion products on Cu exposed in urban, rural/coastal, and hot spring areas in Japan.[21,22] The significant distribution of Cl would indicate that Cl had preferentially diffused into the bulk of the corrosion layers,[23-26] but did not react to form a crystalline or chemical compound within the corrosion film. The relatively small atomic radii of Cl^- ions may make it easier for transport along structural defects, grain boundaries, or dislocations[23] which in turn may provide a path for diffusion of Cu to diffuse to the surface. Establishing the exact role of Cl is beyond the scope of this paper, although studies in our group will aim to identify the role Cl plays in the corrosion of copper.

Conclusions

The corrosion products of Cu exposed to the MFG level III were investigated using different techniques. The weight gain measured after each exposure was compared with the weight gain calculated from the cathodic reduction of the corrosion layers and cross sectioning using an FIB. The results show a relatively good correlation between the measured and the calculated experimental values of weight gain. As expected, within the first week the different corrosion layers thickened until they formed a thick layer that became the determining step for further growth. The corrosion layer is a complex multilayered structure, consisting of (Cu_2O), (CuO), (Cu_2S), (CuS), and preliminary evidence of ($3CuO\ SO_3\ 2H_2O$). No Cl-containing corrosion products (as a chemical compound) were identified in any of the corrosion layers. However, Cl was distributed throughout the corrosion product, indicating that Cl plays an important role in the accelerated MFG class III test.

Acknowledgments

The financial support for this work is through the Science Foundation Ireland under grant number 03/CE3/I405. M. Reid is indebted to the Materials and Surface Science Institute (MSSI) at the University of Limerick for the use of analytical equipment.

The University of Limerick assisted in meeting the publication costs of this article.

References

1. W. H. Abbott, *IEEE Trans. Compon., Hybrids, Manuf. Technol.*, **11**, 22 (1988).
2. W. H. Abbott, *IEEE Trans. Compon., Hybrids, Manuf. Technol.*, **13**, 40 (1990).
3. ASTM International, Standard Guide for Mixed Flowing Gas Tests for Electrical Contacts, ASTM B 845–97 (2003).
4. Telcordia Technologies, NEBS Requirements: Physical Protection, Generic Requirements GR-63-CORE, 2002. Method 5.5.2.
5. R. J. Geckle and R. S. Mroczkowski, *IEEE Trans. Compon., Hybrids, Manuf. Technol.*, **14**, 162 (1991).
6. D. C. Abbott, *IEEE Trans. Compon., Packag., Manuf. Technol., Part C* **22**, 99 (1999).
7. R. Martens and M. Pecht, *J. Mater. Sci. Mater. Electron.*, **11**, 209 (2000).
8. R. Martens and M. G. Pecht, *IEEE Trans. Adv. Packag.*, **23**, 561 (2000).
9. C. Hillman, B. Castillo, and M. Pecht, *Microelectron. Reliab.*, **43**, 635 (2003).
10. P. Zhao and M. Pecht, *Microelectron. Reliab.*, **43**, 775 (2003).
11. P. Zhao and M. Pecht, *IEEE Trans. Device Mater. Reliab.*, **5**, 268 (2005).
12. T. T. M. Tran, C. Fiaud, and E. M. M. Sutter, *Corros. Sci.*, **47**, 1724 (2005).
13. M. Reid, J. Punch, C. Ryan, L. F. Garfias, S. Belochapkine, J. P. Franey, G. E. Derkits, and W. D. Reents, *J. Electrochem. Soc.*, **154**, C209 (2007).
14. W. E. Campbell and U. B. Thomas, Trans. ECS, **76**, 303 (1939).
15. R. H. Lambert and D. J. Trevoy, *J. Electrochem. Soc.*, **105**, 18 (1958).
16. B. I. Rickett and. J. H. Payer, *J. Electrochem. Soc.*, **142**, 3713 (1995).
17. S. J. Krumbien, B. Newell, and V. Pascucci, *J. Test. Eval.*, **11**, 357 (1989).
18. S. Nakayama, T. Kaji, M. Shibata, T. Notoya, and T. Osakai, *J. Electrochem. Soc.*, **154**, C1 (2007).
19. S. K. Chawla, B. I. Rickett, N. Sankarraman, and J. H. Payer, *Corros. Sci.*, **33**, 1617 (1992).
20. K. Nassau, A. E. Miller, and T. E. Graedel, *Corros. Sci.*, **27**, 703 (1987).
21. M. Watanabe, M. Tomita, and T. Ichino, *J. Electrochem. Soc.*, **148**, B522 (2001).
22. M. Watanabe, Y. Higashi, and T. Ichino, *J. Electrochem. Soc.*, **150**, B37 (2003).
23. R. L. Opila, *Corros. Sci.*, **27**, 685 (1987).
24. J. H. Payer, G. Ball, B. I. Rickett, and H. S. Kim, *Mater. Sci. Eng.*, **A198**, 91 (1995).
25. M. Lenglet, J. Lopitaux, C. Leygraf, I. Odnevall, M. Carballeira, J. C. Noualhaguet, J. Guinement, J. Gautier, and J. Boissel, *J. Electrochem. Soc.*, **142**, 3690 (1995).
26. J. P. Franey and M. E. Davis, *Corros. Sci.*, **27**, 659 (1987).